

## §6. Observation of $T_i$ Increase in the ECRH Heated Plasmas in the LHD

Takahashi, H., Nagaoka, K., Nakano, H., Osakabe, M., Morita, S., Goto, M., Oishi, T., Yamada, I., Ido, T., Shimizu, A., Yokoyama, M., Takeiri, Y., Mutoh, T., Murakami, S. (Kyoto Univ.), Pablant, N. (PPPL)

In the 17th experimental campaign of the LHD, increase of  $T_i$  was found in the ECRH heated plasmas. Figure 1 shows the typical time evolution of (a) ECRH power  $P_{\text{ECRH}}$ , (b) the central electron temperature  $T_{e0}$ , (c) the central ion temperature  $T_{i\_crystal}$  measured using the crystal spectroscopy and (d) the line averaged electron density  $n_{e\_fir}$ . The experiment was carried out under the magnetic

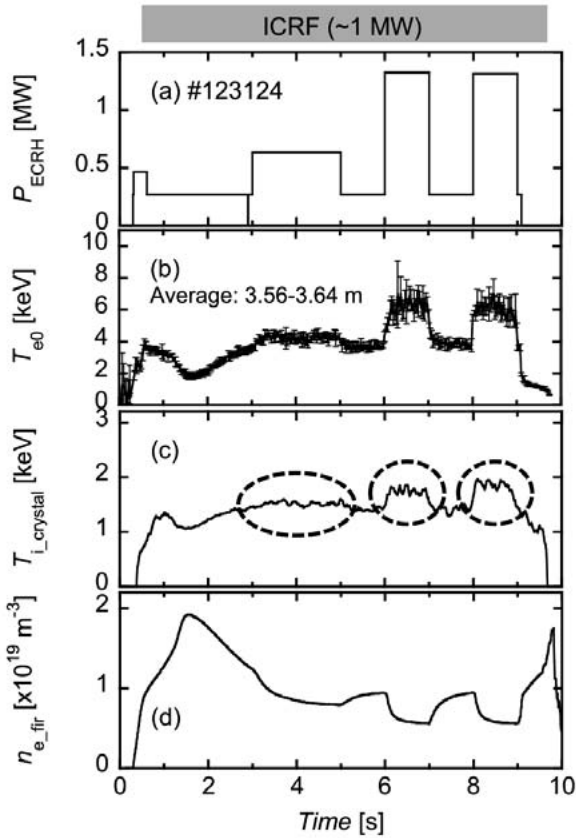


Figure 1. The typical time evolution of (a)  $P_{\text{ECRH}}$ , (b)  $T_{e0}$ , (c)  $T_{i\_crystal}$  and (d)  $n_{e\_fir}$ . The plasma was sustained using 0.27 MW ECRH and  $\sim 1$  MW ICRF and the additional ECRHs were superimposed during 3-5 s (0.37 MW), 6-7 s (1 MW) and 8-9 s (1 MW).

configuration of  $R_{ax} = 3.6$  m,  $B_t = -2.75$  T. In fig.1 (b),  $T_{e0}$  was evaluated as the averaged  $T_e$  value around the magnetic axis. In the discharge, the plasma was sustained using 0.27 MW ECRH and  $\sim 1$  MW ICRF and the additional ECRHs were superimposed during 3-5 s (0.37 MW), 6-7 s (1 MW) and 8-9 s (1 MW). Clear increase of  $T_i$  was observed due to the additional ECRH and the increment of  $T_i$  became larger with increase of additional ECRH power. Note that the  $n_{e\_fir}$  was decreased by the additional ECRH because of the density clumping effect and the drop of  $n_{e\_fir}$  became larger with the higher  $P_{\text{ECRH}}$ . Thus the density normalized ECRH power became considerably large in the high  $P_{\text{ECRH}}$  condition.

Relatively high  $T_i$  plasmas using ECRH were also realized in the discharges with ECRH alone. Figure 2 shows the dependence of  $T_{i\_crystal}$  on the ECRH power normalized by the line averaged electron density  $P_{\text{ECRH}}/n_{e\_fir}$ . The open triangles and the solid circles represent the data in the combination of ICRF and ECRH and ECRH alone, respectively. In the case of ICRF and ECRH mix, there are several data with different  $P_{\text{ECRH}}$  and  $n_{e\_fir}$ . On the other hand,  $P_{\text{ECRH}}$  was fixed value of 4.5 MW and the  $n_{e\_fir}$  was scanned in the case of ECRH alone. The central  $T_i$  extended with increase of  $P_{\text{ECRH}}/n_{e\_fir}$ . Also the  $T_e$  was increased with  $P_{\text{ECRH}}/n_{e\_fir}$ . The increase rate with  $P_{\text{ECRH}}/n_{e\_fir}$  was larger for  $T_e$  than  $T_i$ . It means that both  $T_e$  and  $T_i$  increased with  $T_e/T_i$  in the operational regime. Finally we achieved  $T_{i\_crystal} \sim 4.3$  keV and  $T_{e0} \sim 17$  keV simultaneously for the ECRH plasma with  $n_{e\_fir} \sim 0.2 \times 10^{19} \text{ m}^{-3}$ .

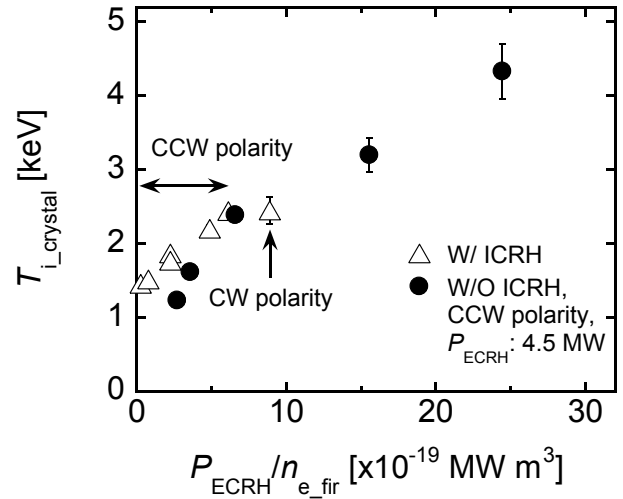


Figure 2. The dependence of  $T_{i\_crystal}$  on  $P_{\text{ECRH}}/n_{e\_fir}$ . The open triangles and the solid circles represent the data in the combination of ICRF and ECRH and ECRH alone, respectively.